The Two-Step Non-Data-Aided SNR Estimation in the Low SNR Region of OFDM Signals

DONG WANG
Nankai University
College of Computer and
Control Engineering
Wei Jin Road, 94, Tianjin
China
nkwangdong@163.com

WEI XU
Tianjin Polytechnic University
Institute of Electronics and
Information Engineering
West Binshui Road, 399, Tianjin
China
doctorxw@126.com

Abstract: In this paper, a novel two-step non-data-aided (NDA) signal to noise ratio (SNR) estimator is proposed to improve its accuracy in the low SNR region of orthogonal frequency division multiplexing (OFDM) signals. The two-step estimator consists of a coarse estimation followed by a refinement step. In the first step, three linear independent coarse estimations of the signal and noise power are obtained by exploring the cyclic-prefix (CP)-induced redundancy. In the second step, these three coarse estimations are refined by resorting to the best linear unbiased estimator (BLUE). Compared with the schemes which only rely on two out of these three coarse estimations, a more accurate SNR estimation can be obtained in the low SNR region. Simulation results show that the proposed noise and signal power estimator achieve approximately 6dB and 2dB SNR gain respectively in the low SNR region, therefore, the proposed SNR estimator provides approximately 4dB SNR gain.

Key–Words: Low SNR, non-data-aided, OFDM, SNR estimation

1 Introduction

The accurate non-data-aided (NDA) signal to noise ratio (SNR) estimation in the low SNR region is crucial to improve the performance of the orthogonal frequency division multiplexing (OFDM) system [1, 2, 3, 4, 5] . The decreased estimation accuracy of the SNR may significantly affect the bit error rate performance of the OFDM systems [6] . Thus, it is essential to investigate the NDA schemes that can improve the accuracy of the SNR estimation in the low SNR region.

The NDA estimator of the SNR is preferred over the data-aided ones primarily due to the fact that the NDA estimator does not require any excess overheads. The existing NDA SNR estimators of OFDM signals may be divided into two categories: the guard-band based [7, 8] and the cyclic-prefix (CP)-based [9, 10, 11] . The CP-based estimators are preferred since the guard-band is easily affected by the attenuation of the low-pass filters and the leakage of data subcarriers [12] .

A number of CP-based NDA SNR estimators are proposed in recent years [9, 10, 11] . However, in the low SNR region these schemes may no longer be effective [11] . For example, the performance of the estimator proposed in [9] depends on the choice of a threshold level which is hard to be obtained especially under the low SNR region. An estimator is introduced in [10] whose performance deteriorates dramatically in the low SNR region and there exists a performance gap in the high SNR region. The estimator [11] bridges the gap, however, with a cost of more serious performance deterioration in the low SNR region.

In this paper, a novel two-step NDA SNR estimator is proposed to improve its accuracy in the low SNR region of OFDM signals. The two-step estimator consists of a coarse estimation step followed by a refinement step. In the first step, three linear independent coarse estimations of the signal and noise power are obtained by exploring the CP-induced redundancy. In the second step, these three coarse estimations are refined by resorting to the best linear unbiased estimator (BLUE). Compared with the schemes [9, 10, 11] which only rely on two out of these three coarse estimations, a more accurate SNR estimation can be obtained in the low SNR region. Simulation results show that the proposed noise and signal power estimator achieve approximately 6dB and 2dB SNR gain respectively in the low SNR region, therefore, the proposed SNR estimator provide approximately 4dB SNR gain.

The rest of this paper is organized as follows. In Sect.2 , the system model for a typical OFDM system is described. In Sect.3 , the two-step SNR esti-

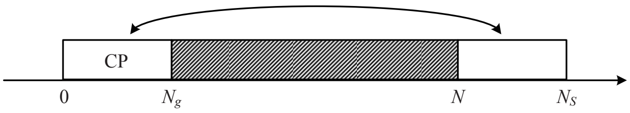

Figure 1: The structure of a transmitted OFDM symbol.

mation scheme is proposed. Simulation results and performance comparisons are given in Sect.4 . Finally, Sect.5 ends this paper with conclusion.

2 Problem Formulation

Consider a base-band equivalent discrete OFDM system comprising of N subcarriers. For $0 \le m \le M-1$, the m-th OFDM symbol of the transmitted signal with normalized power can be represented as

$$x_m(n) = \frac{1}{\sqrt{N}} \sum_{k=0}^{N-1} X_m(k) \exp(j2\pi \frac{k}{N} n) \quad (1)$$

for $n \in \{0, \dots, N-1\}$. $X_m(k)$ is the transmitted complex data symbol at the k-th subcarrier of the m-th OFDM symbol. Without loss of generality, $X_m(k)$ for $0 \le k \le N-1$ are assumed to be independently and identically distributed random variables with normalized variance. The last $N_{\rm g}$ samples of each OFDM symbol are copied and inserted at the front of this symbol as the CP. After adding the CP, the length of $x_m(n)$ extends to $N_{\rm s} = N + N_{\rm g}$ which is shown in Fig.1. The final transmitted signal is given by

$$x(n_1) = \sum_{m=0}^{M-1} x_m(n_1 - mN_{\rm s}) \mathrm{Rect}(n_1 - mN_{\rm s}) \quad (2)$$

where

$$\mathrm{Rect}(n_2) = \begin{cases} 1, & 0 \le n_2 \le N_{\rm s} - 1 \\ 0, & \text{otherwise} \end{cases} \quad (3)$$

is the rectangular pulse function and $n_1 \in [0, MN_{\rm s}–1]$.

Throughout this paper, we assume that the signal $x(n_1)$ is transmitted through a time-invariant Rayleigh fading channel whose channel impulse response is $\{h(l)\}_{l=0,1,\dots,L}$ where the channel order L is assumed to be less than $N_{\rm g}$. Furthermore, we assume that the perfect synchronization is achieved at the receiver [13]. Thus, the received OFDM signal after sampling can be represented as

$$y(n_1) = \sum_{l=0}^{L} h(l) x(n_1 - l) + w(n_1) \quad (4)$$

where $w(n_1) \sim \mathcal{CN}(0, \sigma^2)$ is the white Gaussian noise. The received signal $y(n_1)$ can be modeled approximately as a complex Gaussian random variable when N is large according to the central limit theorem. Let $y_m(n) = y(n + mN_{\rm s})$ for $0 \le n \le N_{\rm s} - 1$ denotes the m-th received OFDM symbol corresponding to $x_m(n)$, whose first L samples are interfered by $x_{m-1}(n)$. The average SNR at the receiver is defined as

$$\mathrm{SNR} = \frac{S}{\sigma^2} \quad (5)$$

where the signal power $S = \sum_{l=0}^{L} |h(l)|^2$ is the received signal power without noise. The vector $\boldsymbol{\theta} = [S, \sigma^2]^{\rm T}$ is the unknown parameter vector and $E_{\rm y} = S + \sigma^2$ represents the total received power. In this paper, we develop a novel scheme to estimate the average SNR at the receiver in the low SNR region.

3 Proposed SNR Estimation Method

Following the procedures suggested by [1, 9], signal and noise power estimation $\hat{S}$ and $\hat{\sigma}^2$ can be retrieved from the CP $\{y_m(n), 0 \le n \le N_{\rm g} - 1\}$ and $\{y_m(n), N \le n \le N_{\rm s} - 1\}$ (blank region in Fig.1). The estimation of the total received power $\hat{E}_{\rm y}$ can be obtained by the second sample moment of the middle part of $y_m(n)$ (shade region). These three estimations $\{\hat{S}, \hat{\sigma}^2, \hat{E}_{\rm y}\}$ are linearly independent since they are retrieved from different parts of the OFDM symbols.

To carefully examine the schemes of the CP-based NDA SNR estimation of OFDM signals [1, 9, 10, 11, 14], we conclude that all of them only use two out of the three estimations $\{\hat{S}, \hat{\sigma}^2, \hat{E}_{\rm y}\}$ to produce the estimation of $\boldsymbol{\theta}$. For example, $\{\hat{S}, \hat{\sigma}^2\}$ are used in [1, 10, 14], and $\{\hat{\sigma}^2, \hat{E}_{\rm y}\}$ are used in [9, 11]. The information contained in the unemployed estimation may be wasted.

In this paper, we propose a new two-step NDA estimator that refines these three coarse estimations $\{\hat{S}, \hat{\sigma}^2, \hat{E}_{\rm y}\}$ jointly by resorting to the BLUE. Compared with the schemes without refinement, a more accurate SNR estimation can be obtained in the low SNR region.

3.1 Two-Step SNR Estimator

In the first step, three coarse estimations of the signal and noise power are obtained by exploring the CP-induced redundancy. In the second step, these estimations are refined jointly by resorting to the BLUE.

Step 1. Coarse Estimation Step

First, the channel order estimation $\hat{L}$ is obtained by (22) of [15] whose formulae are listed in (22)-(26) of Appendix A. As we have $x_m(n) = x_m(n+N)$ for $0 \le n \le N_{\rm g} - 1$, following the procedures suggested by [1, 9], the *coarse estimations* are obtained by

$$\hat{S} = \frac{1}{MN_{\rm g}} \sum_{m=0}^{M-1} \sum_{n=0}^{N_{\rm g}+\hat{L}-1} \Re e[y_m(n) y_m^*(n+N)] \quad (6)$$

$$\hat{\sigma}^2 = \frac{1}{2M(N_{\rm g} - \hat{L})} \sum_{m=0}^{M-1} \sum_{n=\hat{L}}^{N_{\rm g}-1} |y_m(n) - y_m(n+N)|^2 \quad (7)$$

$$\hat{E}_{\rm y} = \frac{1}{M(N-N_{\rm g})} \sum_{m=0}^{M-1} \sum_{n=N_{\rm g}}^{N-1} |y_m(n)|^2 \quad (8)$$

where $(\cdot)^*$ represents the complex conjugate and $\Re e$ represents the real part of a complex quantity. Supposing $\hat{L}$ is a perfect estimation, all of these coarse estimations are unbiased.

Step 2. Refinement Step

The coarse estimations $\{\hat{S}, \hat{\sigma}^2, \hat{E}_{\rm y}\}$ can be used as three observations on the unknown parameter vector $\boldsymbol{\theta} = [S, \sigma^2]^{\rm T}$. Define coarse estimation vector $\hat{\boldsymbol{\theta}}_{\rm c} = [\hat{S}, \hat{\sigma}^2, \hat{E}_{\rm y}]^{\rm T}$. The linear observation model can be represented in matrix form

$$\hat{\boldsymbol{\theta}}_{\rm c} = \mathbf{H}\boldsymbol{\theta} + \mathbf{n} \quad (9)$$

where $\mathbf{H}$ and $\mathbf{n}$ represent the observation matrix and observation noise vector respectively which are defined as

$$\mathbf{H} = \begin{bmatrix} 1 & 0 \\ 0 & 1 \\ 1 & 1 \end{bmatrix}, \quad \mathbf{n} = \begin{bmatrix} \hat{S} - S \\ \hat{\sigma}^2 - \sigma^2 \\ \hat{E}_{\rm y} - E_{\rm y} \end{bmatrix}. \quad (10)$$

Resorting to the BLUE [16], we can obtain an unbiased estimation of $\boldsymbol{\theta}$ with minimized variance under the restriction of linear transformation

$$\hat{\boldsymbol{\theta}}_{\rm r} = (\mathbf{H}^{\rm T}\mathbf{C}^{-1}\mathbf{H})^{-1}\mathbf{H}^{\rm T}\mathbf{C}^{-1}\hat{\boldsymbol{\theta}}_{\rm c} \quad (11)$$

where $\hat{\boldsymbol{\theta}}_{\rm r} = [\hat{S}_{\rm r}, \hat{\sigma}_{\rm r}^2]^{\rm T}$ is the *refined estimation vector* and $\mathbf{C}$ is the covariance matrix of $\hat{\boldsymbol{\theta}}_{\rm c}$.

As $\{\hat{S}, \hat{\sigma}^2\}$ and $\hat{E}_{\rm y}$ are derived from different parts of each $y_m(n)$, we have $\mathrm{cov}(\hat{\sigma}^2, \hat{E}_{\rm y}) = 0$ and $\mathrm{cov}(\hat{S}, \hat{E}_{\rm y}) \approx 0$ [1]. Then $\mathbf{C}$ becomes

$$\mathbf{C} = \begin{bmatrix} \mathrm{var}(\hat{S}) & \mathrm{cov}(\hat{S}, \hat{\sigma}^2) & 0 \\ \mathrm{cov}(\hat{S}, \hat{\sigma}^2) & \mathrm{var}(\hat{\sigma}^2) & 0 \\ 0 & 0 & \mathrm{var}(\hat{E}_{\rm y}) \end{bmatrix}. \quad (12)$$

[1] In view of (6) and (8), there are $\hat{L}$ samples overlapping in each $y_m(n)$ between $\hat{S}$ and $\hat{E}_{\rm y}$. For a typical OFDM system where $\hat{L} \approx L < N_{\rm g} \ll N$, the correlation caused by these $\hat{L}$ samples overlapping can be neglected.

In the low SNR region where $S \ll \sigma^2$, we have

$$\mathrm{cov}(\hat{S}, \hat{\sigma}^2) \approx -\frac{\sigma^4}{2MN_{\rm g}} \quad (13)$$

$$\begin{bmatrix} \mathrm{var}(\hat{S}) \\ \mathrm{var}(\hat{\sigma}^2) \\ \mathrm{var}(\hat{E}_{\rm y}) \end{bmatrix} \approx \begin{bmatrix} (N_{\rm g} + \hat{L})(E_{\rm y}^2 + S^2)/(2MN_{\rm g}^2) \\ \sigma^4/[M(N_{\rm g} - \hat{L})] \\ E_{\rm y}^2/[M(N-N_{\rm g})] \end{bmatrix}. \quad (14)$$

The proofs of (13) and (14) are given in Appendix B. In practice, $\mathbf{C}$ is computed by substituting (13) and (14) into (12) with $\left[S, \sigma^2, E_{\rm y}\right] \approx \left[\hat{S}, \hat{\sigma}^2, \hat{E}_{\rm y}\right]$. Finally, we can obtain the refined SNR estimation through $\hat{\boldsymbol{\theta}}_{\rm r}$ of (11)

$$\hat{\mathrm{SNR}} = \frac{\hat{S}_{\rm r}}{\hat{\sigma}_{\rm r}^2}. \quad (15)$$

The proposed two-step SNR estimator based on the BLUE may be summarized as follows:

Step 1. Coarse Estimation Step

- Compute $\hat{L}$ from (22).
- Substituting $\hat{L}$ into (6), (7) and (8), we obtain the coarse estimation vector $\hat{\boldsymbol{\theta}}_{\rm c} = [\hat{S}, \hat{\sigma}^2, \hat{E}_{\rm y}]^{\rm T}$.

Step 2. Refinement Step

- Compute $\mathbf{C}$ from (12), (13) and (14).
- Substituting $\mathbf{C}$ and $\hat{\boldsymbol{\theta}}_{\rm c}$ into (11), we obtain the refined estimation vector $\hat{\boldsymbol{\theta}}_{\rm r} = [\hat{S}_{\rm r}, \hat{\sigma}_{\rm r}^2]^{\rm T}$.
- Substituting $\{\hat{S}_{\rm r}, \hat{\sigma}_{\rm r}^2\}$ into (15), we obtain the refined SNR estimation $\hat{\mathrm{SNR}}$.

3.2 Performance Analysis

According to the BLUE, the covariance matrix of $\hat{\boldsymbol{\theta}}_{\rm r}$ can be obtained by (derived in Appendix C)

$$\begin{aligned} \mathbf{C}_{\rm r} &= (\mathbf{H}^{\rm T}\mathbf{C}^{-1}\mathbf{H})^{-1} \\ &= \begin{bmatrix} \mathrm{var}(\hat{S}) - A_1 & \mathrm{cov}(\hat{S}, \hat{\sigma}^2) - B \\ \mathrm{cov}(\hat{S}, \hat{\sigma}^2) - B & \mathrm{var}(\hat{\sigma}^2) - A_2 \end{bmatrix} \end{aligned} \quad (16)$$

where

$$A_1 = \frac{\left[\mathrm{var}(\hat{S}) + \mathrm{cov}(\hat{S}, \hat{\sigma}^2)\right]^2}{\mathrm{var}(\hat{S} + \hat{\sigma}^2) + \mathrm{var}(\hat{E}_{\rm y})} \ge 0, \quad (17)$$

$$A_2 = \frac{\left[\mathrm{var}(\hat{\sigma}^2) + \mathrm{cov}(\hat{S}, \hat{\sigma}^2)\right]^2}{\mathrm{var}(\hat{S} + \hat{\sigma}^2) + \mathrm{var}(\hat{E}_{\rm y})} \ge 0 \quad (18)$$

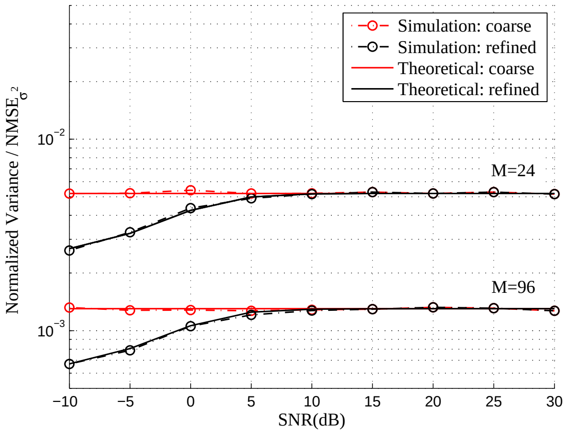

Figure 2: The comparison of the normalized variance between the coarse and refined estimation of the noise power. The simulation parameters are described in Sect.4. In this simulation, $\hat{L}$ is supposed to be a perfect estimation of $L=8$.

and

$$B = \sqrt{A_1 A_2}\,. \tag{19}$$

Then the variance of the refined estimation $\hat{\boldsymbol{\theta}}_{\mathrm{r}}$ is

$$\mathrm{var}(\hat{\boldsymbol{\theta}}_{\mathrm{r}}) = [\mathbf{C}_{\mathrm{r}}]_{ii} = \begin{bmatrix} \mathrm{var}(\hat{S}) - A_1 \\ \mathrm{var}(\hat{\sigma}^2) - A_2 \end{bmatrix} \tag{20}$$

where $[\mathbf{C}_{\mathrm{r}}]_{ii}$ denote the elements on the diagonal of $\mathbf{C}_{\mathrm{r}}$. Compared with the coarse estimation $[\hat{S}, \hat{\sigma}^2]^{\mathrm{T}}$, the refined estimation $\hat{\boldsymbol{\theta}}_{\mathrm{r}} = [\hat{S}_{\mathrm{r}}, \hat{\sigma}_{\mathrm{r}}^2]^{\mathrm{T}}$ has smaller estimation variance where the decrement is

$$\Delta = \begin{bmatrix} \mathrm{var}(\hat{S}) \\ \mathrm{var}(\hat{\sigma}^2) \end{bmatrix} - \begin{bmatrix} \mathrm{var}(\hat{S}_{\mathrm{r}}) \\ \mathrm{var}(\hat{\sigma}_{\mathrm{r}}^2) \end{bmatrix} = \begin{bmatrix} A_1 \\ A_2 \end{bmatrix} \geq 0\,. \tag{21}$$

Simulation results for the comparison of the coarse and refined noise power estimation are presented in Fig.2 . In view of (14) and (20) , the theoretical normalized estimation variance for $\hat{\sigma}^2$ and $\hat{\sigma}_{\mathrm{r}}^2$ (solid lines) are defined as $\mathrm{var}(\hat{\sigma}^2)/\sigma^4$ and $\mathrm{var}(\hat{\sigma}_{\mathrm{r}}^2)/\sigma^4$ respectively. The Monte Carlo simulation results (dash lines) are also provided. In this simulation, $\hat{L}$ is supposed to be a perfect estimation of $L = 8$. The normalized mean square errors (NMSE) for $\hat{\sigma}^2$ and $\hat{\sigma}_{\mathrm{r}}^2$ are defined as $\mathrm{NMSE}_{\sigma^2} = \mathrm{E}[(\hat{\sigma}^2 - \sigma^2)^2]/\sigma^4$ and $\mathrm{NMSE}_{\sigma_{\mathrm{r}}^2} = \mathrm{E}[(\hat{\sigma}_{\mathrm{r}}^2 - \sigma^2)^2]/\sigma^4$ respectively. It can be seen from Fig.2 that the proposed refined estimation (black curve) can achieve better performance in the low SNR region compared with the coarse estimation (red curve).

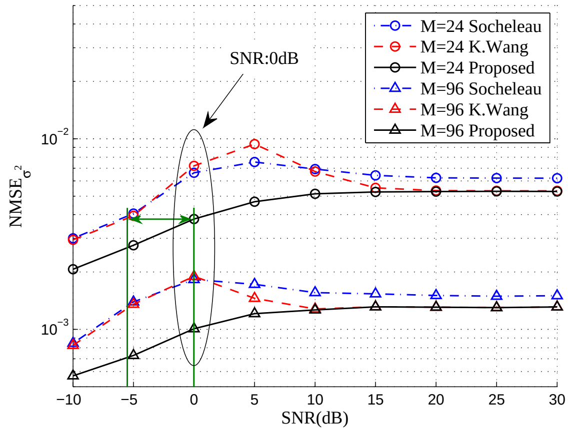

Figure 3: The NMSE of the noise power estimation.

4 Simulations

In this section, we provide simulation results to demonstrate the performance of the proposed algorithm. Compared with the schemes proposed by Socheleau [10] and K.Wang [11] , simulation results show that the NMSEs of the proposed noise and signal power estimator achieve approximately 6dB and 2dB SNR gain in the low SNR region respectively, therefore, the proposed SNR estimator obtains approximately 4dB SNR gain.

A typical OFDM system is considered using QPSK constellation with $N=64$ and $N_{\mathrm{g}}=16$. The channel is assumed to be a nine-tap Rayleigh fading channel with the exponential-decay power delay profile as $\mathrm{E}(|h(l)|^2) = e^{-l/3}\,, 0 \leq l \leq 8$. All results are obtained by averaging over 10^5 independent Monte Carlo trials. A typical low SNR (0dB) is emphasized in each figures with an ellipse in order to clearly demonstrate the improvement of our estimators.

Fig.3 presents the NMSE of the proposed noise power estimation compared with the schemes proposed by Socheleau [10] and K.Wang [11] . It shows that the proposed estimator (black curves) outperforms the other two estimators (blue and red curves) in the low SNR region. Significant improvement occurs in the low SNR region where the proposed estimator achieves approximately 6dB SNR gain indicated by green arrows. The curious phenomenon that the accuracy of $\hat{\sigma}^2$ goes better when SNR drops below 0dB comes from the fact that $\hat{L}$ is always under-estimated (i.e., $\hat{L} < L$) in the low SNR region. In this case, more noise-predominant samples are used in the noise variance estimation, which results in the better performance [11].

Fig.4 compares the signal power estimation per-

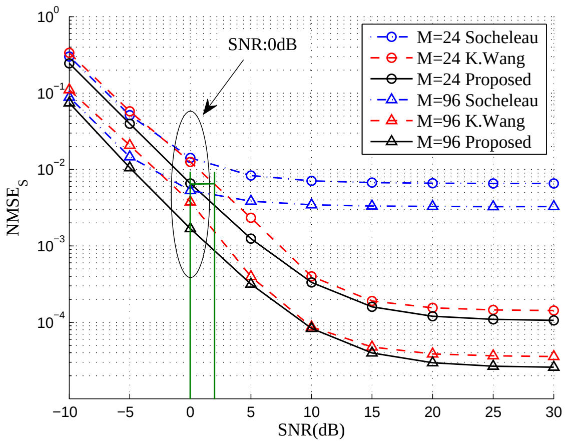

Figure 4: The NMSE of the signal power estimation.

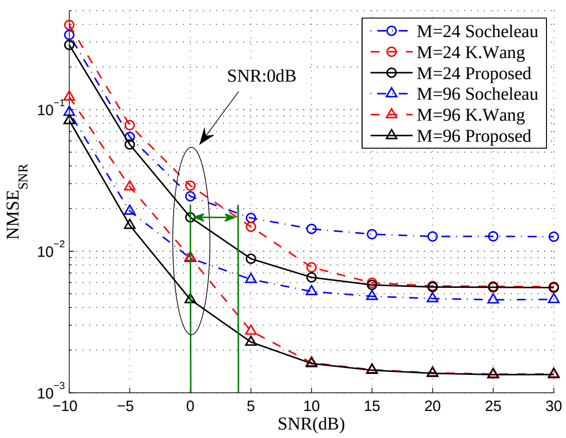

Figure 5: The NMSE of the SNR estimation.

formance of these algorithms. The NMSEs for $\hat{S}$ and $\hat{S}_{\rm r}$ are defined as $\text{NMSE}_S = \text{E}[(\hat{S} - S)^2]/S^2$ and $\text{NMSE}_{S_{\rm r}} = \text{E}[(\hat{S}_{\rm r} - S)^2]/S^2$ respectively. It can be seen from Fig.4 that the proposed scheme (black curves) outperforms the other two (blue and red curves) in all SNR region. In the low SNR region, it achieves approximately 2dB SNR gain (green lines).

In Fig.5, the NMSE of the SNR estimation is defined as $\text{NMSE}_{\text{SNR}} = \text{E}[(\hat{\text{SNR}} - \text{SNR})^2]/\text{SNR}^2$. Since the more accurate estimations for both noise and signal power are obtained, our SNR estimator achieves better performance than the schemes proposed by Socheleau [10] and K.Wang [11]. Compared with these two schemes, the proposed estimator achieves approximately 4dB SNR gain (green arrows) around SNR 0dB.

5 Conclusion

In this paper, a novel two-step NDA SNR estimator is proposed to improve its accuracy in the low SNR region of OFDM signals. The two-step estimator refined the three linear independent coarse estimations of the signal and noise power by resorting to the BLUE. Compared with the schemes without refinement, a more accurate SNR can be obtained in the low SNR region. Simulation results show that the proposed noise power, signal power and SNR estimator achieve approximately 6dB, 2dB and 4dB SNR gain respectively in the low SNR region.

Acknowledgements: The research was supported by the Natural Science Foundation of Tianjin (grant No. 14JCYBJC16100).

References:

[1] B. Sheng, A robust non-data-aided snr estimation method for ofdm systems, *Transactions on Emerging Telecommunications Technologies.* 2013.

[2] F. Harris and C. Dick, Snr estimation techniques for low snr signals, *Wireless Personal Multimedia Communications (WPMC), 2012 15th International Symposium on.* pp.276–280, IEEE, 2012.

[3] ALWADIE, ABDULLAH, Efficient Algorithms for Noise Estimation in Electrical Power Line Communications. *WSEAS Transactions on Communications.* vol 11, no. 11, 2012.

[4] K.S. Sastry and M.P. Babu, Non data aided snr estimation for ofdm signals in frequency selective fading channels, *Wireless Personal Communications.* pp.1–11, 2013.

[5] Devi, B. Rama, K. Kishan Rao, and M. Asha Rani, Bit Error Probability Analysis of Cooperative Relay Selection OFDM Systems Based on SNR Estimation, *In 16th WSEAS International Conference on Computers (part of the 16th CSCC/CSCC 2012), July.* pp. 14-17.

[6] M. Sun, Y. Li, and S. Sun, Impact of snr estimation error on turbo code with high-order modulation, *Vehicular Technology Conference, 2004. VTC 2004-Spring. 2004 IEEE 59th.* pp.1320–1324, IEEE, 2004.

[7] R. Lopez-Valcarce and C. Mosquera, Maximum likelihood snr estimation for asynchronously oversampled ofdm signals, *Signal Processing Advances in Wireless Communications, 2008. SPAWC 2008. IEEE 9th Workshop on.* pp.26–30, IEEE, 2008.

[8] Y. Li, Blind snr estimation of ofdm signals, *Microwave and Millimeter Wave Technology (ICMMT), 2010 International Conference on.* pp.1792–1796, IEEE, 2010.

[9] T. Cui and C. Tellambura, Power delay profile and noise variance estimation for ofdm, *Communications Letters, IEEE.* vol.10, no.1, pp.25–27, 2006.

[10] F.X. Socheleau, A. Aïssa-El-Bey, and S. Houcke, Non data-aided snr estimation of ofdm signals, *Communications Letters, IEEE.* vol.12, no.11, pp.813–815, 2008.

[11] K. Wang and X. Zhang, Blind noise variance and snr estimation for ofdm systems based on information theoretic criteria, *Signal Processing.* vol.90, no.9, pp.2766–2772, 2010.

[12] R. Prasad, *OFDM for wireless communications systems*, Artech House Publishers, 2004.

[13] J.J. Van de Beek, M. Sandell, and P.O. Borjesson, Ml estimation of time and frequency offset in ofdm systems, *Signal Processing, IEEE Transactions on.* vol.45, no.7, pp.1800–1805, 1997.

[14] L. Wilhelmsson, I. Diaz, T. Olsson, and V. O?wall, Analysis of a novel low complex snr estimation technique for ofdm systems, *Wireless Communications and Networking Conference (WCNC), 2011 IEEE.* pp.1646–1651, IEEE, 2011.

[15] D. Wang and J. Zhao, The Non-Data-Aided Noise Variance Estimation in the Low SNR Region of OFDM Signals, *IEICE transactions on communications.* 2015. submitted for publication.

[16] S.M. Kay, *Fundamentals of statistical signal processing, volume i: Estimation theory*, Pearson, 1993.

Appendix A The Estimation of the Channel Order

The channel order estimation adopted in this paper follows the (22) of [15] which is

$$\hat{L} = \underset{0\le j\le N_{\mathrm{g}}-1}{\arg\min} \left\{ \begin{aligned} & 2MN_{\mathrm{s}}\textstyle\sum_{d=j+1}^{N_{\mathrm{g}}} |\hat{\rho}_d|^2 \\ & + 2M\log\left[|\mathbf{R}_j|(\hat{\sigma}_j^2)^{N_{\mathrm{g}}-j}\right] \\ & + 2(j^2+j) \end{aligned} \right\} \quad (22)$$

where we have

$$\hat{\rho}_d = \frac{\sum_{i=0}^{MN_{\mathrm{s}}-d-1} y(i)y^*(i+d)}{\sum_{i=0}^{MN_{\mathrm{s}}-1}|y(i)|^2}\,, \quad (23)$$

$$\mathbf{R}_j = \frac{1}{M}\sum_{m=0}^{M-1}\tilde{\mathbf{y}}_m(1\!:\!j)\tilde{\mathbf{y}}_m^{\mathrm{H}}(1\!:\!j)\,, \quad (24)$$

$$\tilde{\mathbf{y}}_m(1\!:\!j) = [\tilde{y}_m(1), \tilde{y}_m(2), \ldots, \tilde{y}_m(j)]^{\mathrm{T}}\,, \quad (25)$$

$$\hat{\sigma}_j^2 = \frac{1}{M(N_{\mathrm{g}}-j)}\sum_{m=0}^{M-1}\sum_{n=j}^{N_{\mathrm{g}}-1}|\tilde{y}_m(n)|^2 \quad (26)$$

and $\tilde{y}_m(n) = y_m(n) - y_m(n+N)$.

Appendix B Proofs of (13) and (14)

We first derive (13). In view of (6) and (7), the covariance of $\hat{S}$ and $\hat{\sigma}^2$ can be expressed as

$$\mathrm{cov}(\hat{S},\hat{\sigma}^2) = \frac{1}{2M^2N_{\mathrm{g}}(N_{\mathrm{g}}-\hat{L})}\sum_{m_1=0}^{M-1}\sum_{m_2=0}^{M-1}\sum_{n_1=0}^{N_{\mathrm{g}}+\hat{L}-1}\sum_{n_2=\hat{L}}^{N_{\mathrm{g}}-1} \mathrm{cov}\left\{ \begin{aligned} & \Re e\left[y_{m_1}(n_1)y_{m_1}^*(n_1+N)\right], \\ & |y_{m_2}(n_2) - y_{m_2}(n_2+N)|^2 \end{aligned} \right\}. \quad (27)$$

In the low SNR region where $S \ll \sigma^2$, the multipath-induced correlation between the adjacent received samples are quite small. So we keep the dominant path $h(0)$ and ignore the minor multipaths $h(l)\approx 0$ for $1\le l\le L$. As retrieved from different samples, there are $M^2(N_{\mathrm{g}}+\hat{L})(N_{\mathrm{g}}-\hat{L})$ terms in the sum of (27) and all terms are equal to zero except the $M(N_{\mathrm{g}}-\hat{L})$ terms with $m_1 = m_2$ and $n_1 = n_2$ which can be expressed as

$$\Phi = \sum_{m=0}^{M-1}\sum_{n=\hat{L}}^{N_{\mathrm{g}}-1}\mathrm{cov}\left\{ \begin{aligned} & \Re e[y_m(n)y_m^*(n+N)], \\ & |y_m(n) - y_m(n+N)|^2 \end{aligned} \right\}. \quad (28)$$

Assuming $\hat{L}$ is a perfect estimation, we rewrite the received samples for convenient expression

$$\begin{aligned} y_m(n) &= h(0)x_m(n) + w(mN_{\mathrm{s}}+n) \\ &= x + w_1 \\ &= (x_{\mathrm{Re}} + w_{1\mathrm{Re}}) + j(x_{\mathrm{Im}} + w_{1\mathrm{Im}}) \end{aligned} \quad (29)$$

$$\begin{aligned} y_m(n+N) &= h(0)x_m(n) + w(mN_{\mathrm{s}}+n+N) \\ &= x + w_2 \\ &= (x_{\mathrm{Re}} + w_{2\mathrm{Re}}) + j(x_{\mathrm{Im}} + w_{2\mathrm{Im}}) \end{aligned} \quad (30)$$

where $x = h(0)x_m(n) \sim \mathcal{CN}(0,S)$ represents the signal component, $w_1 = w(mN_{\mathrm{s}}+n) \sim \mathcal{CN}(0,\sigma^2)$ and $w_2 = w(mN_{\mathrm{s}}+n+N) \sim \mathcal{CN}(0,\sigma^2)$ represent the noise components. The subscripts $(\cdot)_{\mathrm{Re}}$ and $(\cdot)_{\mathrm{Im}}$ represent the real and imaginary part respectively which have zero-mean, half-variance and are independent with each other.

With the help of (29) and (30), we have

$$\begin{aligned}
&\mathrm{cov}\left\{\begin{matrix}\Re e\,[y_m(n)y_m^*(n+N)]\,,\\ |y_m(n)-y_m(n+N)|^2\end{matrix}\right\}\\
&=\mathrm{cov}\left\{\begin{matrix}x_{\mathrm{Re}}^2+x_{\mathrm{Im}}^2\\ +w_{1\mathrm{Re}}x_{\mathrm{Re}}+w_{2\mathrm{Re}}x_{\mathrm{Re}}\\ +w_{1\mathrm{Im}}x_{\mathrm{Im}}+w_{2\mathrm{Im}}x_{\mathrm{Im}}\\ +w_{1\mathrm{Re}}w_{2\mathrm{Re}}+w_{1\mathrm{Im}}w_{2\mathrm{Im}}\end{matrix}, \begin{matrix}w_{1\mathrm{Re}}^2+w_{2\mathrm{Re}}^2\\ +w_{1\mathrm{Im}}^2+w_{2\mathrm{Im}}^2\\ -2w_{1\mathrm{Re}}w_{2\mathrm{Re}}\\ -2w_{1\mathrm{Im}}w_{2\mathrm{Im}}\end{matrix}\right\}\\
&=\mathrm{cov}(w_{1\mathrm{Re}}x_{\mathrm{Re}},w_{1\mathrm{Re}}^2)-\mathrm{cov}(w_{1\mathrm{Re}}x_{\mathrm{Re}},2w_{1\mathrm{Re}}w_{2\mathrm{Re}})\\
&\quad+\mathrm{cov}(w_{2\mathrm{Re}}x_{\mathrm{Re}},w_{2\mathrm{Re}}^2)-\mathrm{cov}(w_{2\mathrm{Re}}x_{\mathrm{Re}},2w_{1\mathrm{Re}}w_{2\mathrm{Re}})\\
&\quad+\mathrm{cov}(w_{1\mathrm{Im}}x_{\mathrm{Im}},w_{1\mathrm{Im}}^2)-\mathrm{cov}(w_{1\mathrm{Im}}x_{\mathrm{Im}},2w_{1\mathrm{Im}}w_{2\mathrm{Im}})\\
&\quad+\mathrm{cov}(w_{2\mathrm{Im}}x_{\mathrm{Im}},w_{2\mathrm{Im}}^2)-\mathrm{cov}(w_{2\mathrm{Im}}x_{\mathrm{Im}},2w_{1\mathrm{Im}}w_{2\mathrm{Im}})\\
&\quad+\mathrm{cov}(w_{1\mathrm{Re}}w_{2\mathrm{Re}},w_{1\mathrm{Re}}^2)+\mathrm{cov}(w_{1\mathrm{Re}}w_{2\mathrm{Re}},w_{2\mathrm{Re}}^2)\\
&\quad+\mathrm{cov}(w_{1\mathrm{Im}}w_{2\mathrm{Im}},w_{1\mathrm{Im}}^2)+\mathrm{cov}(w_{1\mathrm{Im}}w_{2\mathrm{Im}},w_{2\mathrm{Im}}^2)\\
&\quad-\mathrm{cov}(w_{1\mathrm{Re}}w_{2\mathrm{Re}},2w_{1\mathrm{Re}}w_{2\mathrm{Re}})\\
&\quad-\mathrm{cov}(w_{1\mathrm{Im}}w_{2\mathrm{Im}},2w_{1\mathrm{Im}}w_{2\mathrm{Im}})\,. \qquad (31)
\end{aligned}$$

In (31), all the covariance of obvious independent pairs have been removed, i.e., either any two terms out of $\{x, w_1, w_2\}$ or the real and imaginary part.

In view of (31), we have

$$\begin{aligned}
&\mathrm{cov}(w_{1\mathrm{Re}}x_{\mathrm{Re}},w_{1\mathrm{Re}}^2)\\
&\quad=\mathrm{E}(w_{1\mathrm{Re}}^3x_{\mathrm{Re}})-\mathrm{E}(w_{1\mathrm{Re}}x_{\mathrm{Re}})\mathrm{E}(w_{1\mathrm{Re}}^2)\\
&\quad=\mathrm{E}(w_{1\mathrm{Re}}^3)\mathrm{E}(x_{\mathrm{Re}})-\mathrm{E}(w_{1\mathrm{Re}})\mathrm{E}(x_{\mathrm{Re}})\mathrm{E}(w_{1\mathrm{Re}}^2)\\
&\quad=0\,. \qquad (32)
\end{aligned}$$

Following the same procedure, it can be easily verified that all terms in (31) are equal to zero except the last two terms

$$\begin{aligned}
&\mathrm{cov}(w_{1\mathrm{Re}}w_{2\mathrm{Re}},2w_{1\mathrm{Re}}w_{2\mathrm{Re}})\\
&\quad=2\mathrm{E}(w_{1\mathrm{Re}}^2w_{2\mathrm{Re}}^2)-2\,[\mathrm{E}(w_{1\mathrm{Re}}w_{2\mathrm{Re}})]^2\\
&\quad=2\mathrm{E}(w_{1\mathrm{Re}}^2)\mathrm{E}(w_{2\mathrm{Re}}^2)-2\,[\mathrm{E}(w_{1\mathrm{Re}})\mathrm{E}(w_{2\mathrm{Re}})]^2\\
&\quad=\frac{\sigma^4}{2} \qquad (33)
\end{aligned}$$

and

$$\mathrm{cov}(w_{1\mathrm{Im}}w_{2\mathrm{Im}},2w_{1\mathrm{Im}}w_{2\mathrm{Im}})=\frac{\sigma^4}{2}\,. \qquad (34)$$

Substituting(28), (31), (33) and (34) into (27), we have the covariance of $\hat{S}$ and $\hat{\sigma}^2$

$$\begin{aligned}
\mathrm{cov}(\hat{S},\hat{\sigma}^2)&\approx\frac{M(N_{\mathrm{g}}-\hat{L})}{2M^2N_{\mathrm{g}}(N_{\mathrm{g}}-\hat{L})}\left(-\frac{\sigma^4}{2}-\frac{\sigma^4}{2}\right)\\
&=-\frac{\sigma^4}{2MN_{\mathrm{g}}} \qquad (35)
\end{aligned}$$

in the low SNR region.

In order to derive (14), we first need to prove the following lemma.

Lemma 1. *Let X and Y denote two real Gaussian random variables with zero-mean, equal variance σ_X^2 and correlation coefficient ρ. Then, we have*

$$\begin{aligned}
\mathrm{var}(XY)&=(1+\rho^2)\sigma_X^4\\
&=\sigma_X^4+[\mathrm{cov}(X,Y)]^2\\
&=\sigma_X^4+[\mathrm{E}(XY)]^2\,. \qquad (36)
\end{aligned}$$

Proof: The random variable Y can be expressed as $Y=\rho X+\sqrt{1-\rho^2}Z$ where the random variable $Z\sim\mathcal{N}(0,\sigma_X^2)$ is independent of X. The variance of the product of XY is given by

$$\begin{aligned}
\mathrm{var}(XY)&=\mathrm{var}\left[X\left(\rho X+\sqrt{1-\rho^2}Z\right)\right]\\
&=\mathrm{var}\left(\rho X^2+\sqrt{1-\rho^2}XZ\right)\\
&=\rho^2\mathrm{var}(X^2)+(1-\rho^2)\mathrm{var}(XZ)\\
&\quad+2\rho\sqrt{1-\rho^2}\mathrm{cov}(X^2,XZ)\\
&=\rho^2\left\{\mathrm{E}(X^4)-[\mathrm{E}(X^2)]^2\right\}\\
&\quad+(1-\rho^2)\mathrm{var}(X)\mathrm{var}(Z)\\
&\quad+2\rho\sqrt{1-\rho^2}\mathrm{cov}(X^2,XZ)\\
&=\rho^2(3\sigma_X^4-\sigma_X^4)+(1-\rho^2)\sigma_X^4\\
&\quad+2\rho\sqrt{1-\rho^2}\mathrm{cov}(X^2,XZ)\\
&=(1+\rho^2)\sigma_X^4\\
&\quad+2\rho\sqrt{1-\rho^2}\mathrm{cov}(X^2,XZ) \qquad (37)
\end{aligned}$$

where

$$\begin{aligned}
\mathrm{cov}(X^2,XZ)&=\mathrm{E}\{[X^2-\mathrm{E}(X^2)][XZ-\mathrm{E}(XZ)]\}\\
&=\mathrm{E}[(X^2-\sigma_X^2)XZ]\\
&=\mathrm{E}(X^3-\sigma_X^2X)\mathrm{E}(Z)\\
&=0\,. \qquad (38)
\end{aligned}$$

Substituting (38) into (37), we obtain (36). □

Now we are ready to derive (14).

First, we derive $\mathrm{var}(\hat{S})$. With the low SNR assumption, the products $y_m(n)y_m^*(n+N)$ are mutually independent with each other for different m or n. According to (6), the variance of $\hat{S}$ can be simplified as

$$\begin{aligned}
\mathrm{var}(\hat{S})&=\frac{1}{M^2N_{\mathrm{g}}^2}\mathrm{var}\left\{\sum_{m=0}^{M-1}\sum_{n=0}^{N_{\mathrm{g}}+\hat{L}-1}\Re e[y_m(n)y_m^*(n+N)]\right\}\\
&=\frac{N_{\mathrm{g}}+\hat{L}}{MN_{\mathrm{g}}^2}\mathrm{var}\{\Re e[y_m(n)y_m^*(n+N)]\}\\
&=\frac{N_{\mathrm{g}}+\hat{L}}{MN_{\mathrm{g}}^2}\mathrm{var}\left\{\begin{matrix}(x_{\mathrm{Re}}+w_{1\mathrm{Re}})(x_{\mathrm{Re}}+w_{2\mathrm{Re}})\\ +(x_{\mathrm{Im}}+w_{1\mathrm{Im}})(x_{\mathrm{Im}}+w_{2\mathrm{Im}})\end{matrix}\right\}\\
&=\frac{2(N_{\mathrm{g}}+\hat{L})}{MN_{\mathrm{g}}^2}\mathrm{var}\{(x_{\mathrm{Re}}+w_{1\mathrm{Re}})(x_{\mathrm{Re}}+w_{2\mathrm{Re}})\}. \qquad (39)
\end{aligned}$$

It can be easily verified that $x_{\mathrm{Re}}+w_{1\mathrm{Re}}$ and $x_{\mathrm{Re}}+w_{2\mathrm{Re}}$ are both Gaussian random variables with zero-mean, $E_{\mathrm{y}}/2$ variance. We also have

$$\begin{aligned}&\mathrm{E}\left[(x_{\mathrm{Re}}+w_{1\mathrm{Re}})(x_{\mathrm{Re}}+w_{2\mathrm{Re}})\right]\\&\quad=\mathrm{E}\left(x_{\mathrm{Re}}^2+w_{1\mathrm{Re}}x_{\mathrm{Re}}+w_{2\mathrm{Re}}x_{\mathrm{Re}}+w_{1\mathrm{Re}}w_{2\mathrm{Re}}\right)\\&\quad=\mathrm{E}\left(x_{\mathrm{Re}}^2\right)=S/2\,.\end{aligned}\tag{40}$$

Then according to (36) in lemma 1 , we have

$$\begin{aligned}&\mathrm{var}\left[(x_{\mathrm{Re}}+w_{1\mathrm{Re}})(x_{\mathrm{Re}}+w_{2\mathrm{Re}})\right]\\&\quad=\left[\mathrm{var}(x_{\mathrm{Re}}+w_{1\mathrm{Re}})\right]^2\\&\qquad+\{\mathrm{E}\left[(x_{\mathrm{Re}}+w_{1\mathrm{Re}})(x_{\mathrm{Re}}+w_{2\mathrm{Re}})\right]\}^2\\&\quad=\frac{1}{4}(E_{\mathrm{y}}^2+S^2)\,.\end{aligned}\tag{41}$$

Substituting (41) into (39), the variance of $\hat{S}$ yields

$$\mathrm{var}(\hat{S})=\frac{N_{\mathrm{g}}+\hat{L}}{2MN_{\mathrm{g}}^2}(E_{\mathrm{y}}^2+S^2)\tag{42}$$

in the low SNR region.

Similar to the derivation of $\mathrm{var}(\hat{S})$, in view of (7) and (8) , we can obtain the variance of $\hat{\sigma}^2$ as

$$\begin{aligned}\mathrm{var}(\hat{\sigma}^2)&\approx\frac{1}{4M(N_{\mathrm{g}}-\hat{L})}\mathrm{var}\{|y_m(n)-y_m(n+N)|^2\}\\&=\frac{1}{4M(N_{\mathrm{g}}-\hat{L})}\mathrm{var}\{|w_1-w_2|^2\}\\&=\frac{\sigma^4}{M(N_{\mathrm{g}}-\hat{L})}\end{aligned}\tag{43}$$

and the variance of $\hat{E}_{\mathrm{y}}$ as

$$\begin{aligned}\mathrm{var}(\hat{E}_{\mathrm{y}})&\approx\frac{1}{M(N-N_{\mathrm{g}})}\mathrm{var}\{|y_m(n)|^2\}\\&=\frac{E_{\mathrm{y}}^2}{M(N-N_{\mathrm{g}})}\,.\end{aligned}\tag{44}$$

During the derivations of (43) and (44) , the equation $\mathrm{var}(|X|^2)=\sigma_X^4$ for $X\sim\mathcal{CN}(0,\sigma_X^2)$ is used.

According to (42) , (43) and (44) the variance of the coarse estimation vector in the low SNR region is

$$\begin{bmatrix}\mathrm{var}(\hat{S})\\\mathrm{var}(\hat{\sigma}^2)\\\mathrm{var}(\hat{E}_{\mathrm{y}})\end{bmatrix}\approx\begin{bmatrix}(N_{\mathrm{g}}+\hat{L})(E_{\mathrm{y}}^2+S^2)/(2MN_{\mathrm{g}}^2)\\\sigma^4/[M(N_{\mathrm{g}}-\hat{L})]\\E_{\mathrm{y}}^2/[M(N-N_{\mathrm{g}})]\end{bmatrix}.\tag{45}$$

Appendix C Proof of the Covariance of $\hat{\boldsymbol{\theta}}_{\mathrm{r}}$

In view of (12) , $\mathbf{C}$ is a block diagonal matrix. Thus its inverse matrix is

$$\mathbf{C}^{-1}=\frac{1}{A}\begin{bmatrix}\mathrm{var}(\hat{\sigma}^2)&-\mathrm{cov}(\hat{S},\hat{\sigma}^2)&0\\-\mathrm{cov}(\hat{S},\hat{\sigma}^2)&\mathrm{var}(\hat{S})&0\\0&0&A'\end{bmatrix}\tag{46}$$

where $A=\mathrm{var}(\hat{S})\mathrm{var}(\hat{\sigma}^2)-[\mathrm{cov}(\hat{S},\hat{\sigma}^2)]^2$ and $A'=A/\mathrm{var}(\hat{E}_{\mathrm{y}})$. According to the BLUE, the theoretical covariance of $\hat{\boldsymbol{\theta}}_{\mathrm{r}}$ can be obtained by

$$\begin{aligned}&\mathbf{C}_{\mathrm{r}}=(\mathbf{H}^{\mathrm{T}}\mathbf{C}^{-1}\mathbf{H})^{-1}\\&=A\begin{bmatrix}\mathrm{var}(\hat{\sigma}^2)+A'&-\mathrm{cov}(\hat{S},\hat{\sigma}^2)+A'\\-\mathrm{cov}(\hat{S},\hat{\sigma}^2)+A'&\mathrm{var}(\hat{S})+A'\end{bmatrix}^{-1}\\&=\frac{A}{A+A'\mathrm{var}(\hat{S}+\hat{\sigma}^2)}\begin{bmatrix}\mathrm{var}(\hat{S})+A'&\mathrm{cov}(\hat{S},\hat{\sigma}^2)-A'\\\mathrm{cov}(\hat{S},\hat{\sigma}^2)-A'&\mathrm{var}(\hat{\sigma}^2)+A'\end{bmatrix}\\&=\frac{\begin{bmatrix}\mathrm{var}(\hat{S})\mathrm{var}(\hat{E}_{\mathrm{y}})+A&\mathrm{cov}(\hat{S},\hat{\sigma}^2)\mathrm{var}(\hat{E}_{\mathrm{y}})-A\\\mathrm{cov}(\hat{S},\hat{\sigma}^2)\mathrm{var}(\hat{E}_{\mathrm{y}})-A&\mathrm{var}(\hat{\sigma}^2)\mathrm{var}(\hat{E}_{\mathrm{y}})+A\end{bmatrix}}{\mathrm{var}(\hat{S}+\hat{\sigma}^2)+\mathrm{var}(\hat{E}_{\mathrm{y}})}\\&=\begin{bmatrix}\mathrm{var}(\hat{S})-A_1&\mathrm{cov}(\hat{S},\hat{\sigma}^2)-B\\\mathrm{cov}(\hat{S},\hat{\sigma}^2)-B&\mathrm{var}(\hat{\sigma}^2)-A_2\end{bmatrix}\end{aligned}\tag{47}$$

where $\{A_1,A_2,B\}$ are defined in (17) , (18) and (19) respectively.